Destabilization of magnetosonic-whistler waves by a relativistic runaway beam

G. Pokol 1,2), T. Fülöp 2), P. Helander 3) and M. Lisak 2)

1) Department of Nuclear Techniques, Budapest University of Technology and Economics, Association EURATOM, Budapest, Hungary
2) Department of Radio and Space Science, Chalmers University of Technology, Göteborg, Sweden
3) EURATOM/UKAEA Fusion Association, Culham Science Centre, Abingdon, U.K.

e-mail contact of main author: pokol@reak.bme.hu

Abstract. Magnetosonic-whistler waves may be destabilized by runaway electrons with strongly anisotropic velocity distribution. The unstable wave frequency is well below the non-relativistic electron cyclotron frequency but above the ion cyclotron frequency. The linear instability growth rate of the magnetosonic-whistler wave destabilized by an avalanche of relativistic runaway electrons through the anomalous Doppler-resonance is calculated in a local analysis using the homogenous plasma approximation. The perturbative stability analysis is complemented by numerical solution of the dispersion equation including the full hot plasma dielectric tensor. In the parameter range relevant to disruptions in large tokamaks, the growth rate is largest for nearly perpendicular propagation. By assuming that the dominant damping mechanism in cold post-disruption plasmas is due to collisions, the local threshold of the instability can be shown to depend on the fraction of runaway electrons, the magnetic field and the temperature of the background plasma. The dependence on the magnetic field is consistent with the experimental observations suggesting that there is a critical toroidal magnetic field below which there is no runaway current after a disruption. One reason for this absence of runaways may be that the instability scatters the runaways in pitch-angle and prevents the beam from forming. Indeed, the quasilinear analysis shows that the main result of the instability is pitch-angle scattering of the runaway electrons on a typical time scale of a microsecond.

1. Introduction

The large toroidal electric field induced in a tokamak disruption can generate a beam of highly relativistic runaway electrons with energy of order 20 MeV, which is a potentially serious problem for reactor-scale tokamaks with large currents. In such devices, it is expected that the runaway beam may form particularly easily because of the efficacy of the so-called “runaway avalanche” mechanism [1].

In present experiments, up to about a half the pre-disruption current can be converted to runaways, and it is feared that this fraction will rise in future devices because of avalanching [2]. However, the number of runaway electrons generated varies widely between different disruptions, and several tokamaks have reported that no runaway generation occurs unless the magnetic field exceeds 2.2 T [3, 4, 5]. In the present paper, we explore a possible reason for this observation.

The presence of a runaway beam with strongly anisotropic velocity distribution may cause various kinetic instabilities to appear. Previous works have analyzed a number of such possible instabilities using simple models for the runaway distribution function. Resonant interaction of runaways with lower-hybrid waves was investigated in Refs. [6, 7, 8], and the instability threshold of the upper-hybrid wave driven unstable by runaways was derived in Ref. [9], where it was concluded that this wave is stable in collisional post-disruption plasmas.

We analyze the linear instability of magnetosonic-whistler waves. The unstable wave frequency will be shown to be well below the non-relativistic electron cyclotron frequency ω_{ce} but above the ion cyclotron frequency ω_{ci}. The most important resonant interaction is at the anomalous Doppler resonance $\omega - k_\| v_\| = -\omega_{ce}/\gamma$, where ω is the wave frequency, $k_\|$ and $v_\|$ are the wave number and particle velocity parallel to the magnetic field, and γ is the Lorenz factor. As in Ref. [9] we assume that the dominant damping mechanism in the cold post-disruption plasma is collisional damping, which then determines the instability threshold. When the degree of anisotropy of the runaway distribution function exceeds a critical level, unstable waves are excited, and the interaction with these waves leads to pitch-angle scattering of resonant electrons.

2. Runaway distribution function

In this section we derive the velocity-space distribution function for runaway electrons produced by avalanching. The starting point for this calculation is the kinetic equation for relativistic electrons in homogenous magnetic field, which can be simplified using assumptions valid in tokamak disruptions $E \gg 1$ and $p_\perp \ll p_\| \simeq p$, giving the following form:

$$\tau \frac{\partial f}{\partial t} + (E-1)\frac{\partial f}{\partial p_\|} = \frac{1+Z}{2}\frac{1}{p_\perp}\frac{\partial}{\partial p_\perp} p_\perp \frac{\partial f}{\partial p_\perp}, \tag{1}$$

where $\tau = 4\pi\epsilon_0^2 m_{e0}^2 c^3/n_e e^4 \ln\Lambda$ is the collision time for relativistic electrons, c the speed of light, m_{e0} the electron rest mass, n_e the background electron density, $E = e|E_\||\tau/m_{e0}c$ the normalized parallel electric field, Z the effective ion charge, $p = \gamma v/c$ is the normalized relativistic momentum, and $\gamma = \sqrt{1+p^2}$ the Lorentz factor.

Using the Rosenbluth and Putvinski [1] avalanche growth rate as a boundary condition at low p the solution of equation (1) gives

$$f(p_\|, p_\perp, t) = \frac{C}{p_\|}\exp\left(\frac{(E-1)t/\tau - p_\|}{c_Z} - \frac{\alpha p_\perp^2}{2p_\|}\right), \tag{2}$$

where C is related to the runaway density by $C = (n_r\alpha)/(2\pi c_Z)\exp\left[(E-1)t/(\tau c_Z)\right]$, $c_Z = \sqrt{3(Z+5)/\pi}\ln\Lambda$ and $\alpha = (E-1)/(1+Z)$. A more detailed solution of the equation can be found in Ref. [10].

3. Stability analysis

The dispersion relation for the fast wave is

$$\left(\epsilon_{11} - k_\|^2 c^2/\omega^2\right)\left(\epsilon_{22} - k^2c^2/\omega^2\right) + \epsilon_{12}^2 = 0, \tag{3}$$

where k is the wavenumber and $\boldsymbol{\epsilon} = \mathbf{1} + \boldsymbol{\chi}$ is the dielectric tensor [11]. The $\boldsymbol{\chi}$ susceptibility tensor consists of additive contributions from cold background ions, electrons and energetic runaway electrons.

In the parameter range $\omega_{ci} \ll \omega \ll \omega_{ce}$, $|k| \gg |k_\parallel|$ and $kc \gg \omega_{pi}$, the dispersion relation can be simplified to

$$k^2 v_A^2 \left(1 + \frac{k_\parallel^2 c^2}{\omega_{pi}^2}\right) - \omega^2 \left(1 + \frac{k^2 v_A^2}{\omega_{ci}\omega_{ce}}\right) = \frac{\omega_{ci}^2 \omega^2}{\omega_{pi}^2} \left[\left(1 + \frac{k^2 v_A^2}{\omega_{ci}^2}\right)\chi_{11}^r + \left(1 + \frac{k_\parallel^2 v_A^2}{\omega_{ci}^2}\right)\chi_{22}^r - 2i\frac{\omega}{\omega_{ci}}\chi_{12}^r\right],$$

where ω_{pi} and ω_{pe} are the ion and electron plasma frequencies, $k_\perp$ is the component of the wave vector perpendicular to the magnetic field, $v_A = c\omega_{ci}/\omega_{pi}$ is the Alfvén velocity and the superscript ^{r} denotes the runaway contribution to the dielectric tensor. Given that $\omega_{pe} \gg kc$, χ_{11}^e and χ_{22}^e electron contributions can be neglected. In the frequency range of interest the χ_{22}^r and $i\chi_{12}^r$ terms can also be neglected provided that $k^2 v_A^2 \gg \omega\omega_{ci}$, and the dispersion relation takes the following simple form:

$$k^2 v_A^2 \left(1 + \frac{k_\parallel^2 c^2}{\omega_{pi}^2}\right) - \omega^2 = \omega^2 \frac{k^2 v_A^2}{\omega_{pi}^2}\chi_{11}^r. \tag{4}$$

Without runaways, this equation gives the magnetosonic-whistler dispersion relation $\omega_0 = kv_A\sqrt{1 + k_\parallel^2 c^2/\omega_{pi}^2}$, which reduces to the magnetosonic wave $\omega_0 = kv_A$ for perpendicular propagation ($k_\parallel = 0$) and to the whistler wave $\omega_0 = kk_\parallel v_A^2/\omega_{ci}$ for $k_\parallel^2 c^2/\omega_{pi}^2 \gg 1$.

The remaining runaway contribution to the dielectric tensor is

$$\chi_{11}^r = 2\pi \frac{\omega_{pr}^2 \omega_{ce}^2}{k_\perp^2 \omega c^2} \int_0^\infty dp_\perp \int_{-\infty}^\infty dp_\parallel \sum_{n=-\infty}^{\infty} \frac{\frac{\partial f_r}{\partial p_\perp} + \frac{k_\parallel c}{\omega\gamma}\left(p_\perp \frac{\partial f_r}{\partial p_\parallel} - p_\parallel \frac{\partial f_r}{\partial p_\perp}\right)}{\gamma(\omega - k_\parallel c p_\parallel/\gamma - n\Omega)} n^2 J_n^2(z), \tag{5}$$

where $\omega_{pr} = \sqrt{n_r e^2/m_{e0}\epsilon_0}$ is the non-relativistic runaway electron plasma frequency, J_n is the Bessel function of the first kind and of order n, $\Omega = eB/m_e = \omega_{ce}/\gamma$, $z = k_\perp c p_\perp/\omega_{ce}$ and $f_r = f/n_r$ is the normalized runaway distribution function.

The instability growth rate can be calculated by solving (4) for the runaway distribution (2). For realistic parameters and the frequency region of interest ($\omega_{ci} \ll \omega_0 \ll \omega_{ce}$), only the anomalous Doppler resonance ($n = -1$) has to be taken into account.

3.1. Perturbative analysis

The instability growth rate γ_i for a small perturbation $\omega = \omega_0 + \delta\omega$, where $\gamma_i = \mathrm{Im}\delta\omega$, is given by

$$\frac{\gamma_i}{\omega_0} = -\frac{k^2 v_A^2}{2\omega_{pi}^2}\mathrm{Im}\chi_{11}^r \tag{6}$$

Using the approximation $\gamma \simeq p_\parallel$ valid for the ultra-relativistic runaway tail and substituting the runaway electron distribution from Eq. (2), we obtain:

$$\frac{\gamma_i}{\omega_0} = \frac{\hat{C}}{4a_{-1}^2}\left\{K_\perp^2 K_\parallel (1-y) I_0(\lambda) + \left[2a_{-1}b_{-1} + K_\perp^2 K_\parallel(1-y)\right] I_1(\lambda)\right\} e^\lambda, \tag{7}$$

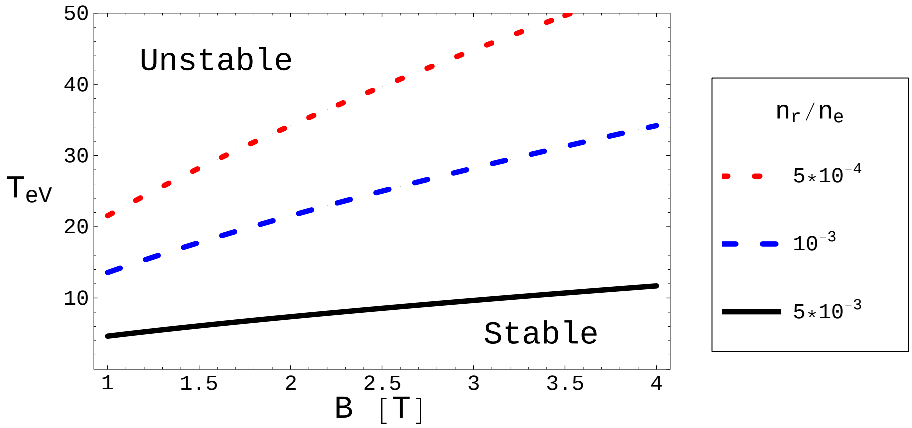

Figure 1: Stability threshold from Eq. (10) for different runaway fractions.

where $y = \omega_0/k_\parallel c$, $K_\perp = k_\perp c/\omega_{ce}$, $K_\parallel = k_\parallel c/\omega_{ce}$, $\lambda = K_\perp^2/(2a_{-1})$, $a_{-1} = \alpha K_\parallel(y-1)/2$, $b_{-1} = \alpha(1-y) - K_\parallel(1-y) - 1/c_Z$, I_n are modified Bessel functions of the first kind and of order n, and $\hat{C} = (1-y)(\pi\alpha\omega_{pr}^2/2c_Z\omega_{pi}^2)(k^2v_A^2/\omega_0^2)(k_\parallel^2/k_\perp^2)\exp\left\{-1/[c_Z K_\parallel(1-y)]\right\}$.

If $\lambda \ll 1$, we can expand the Bessel and exponential functions for small parameters. Assuming that $\alpha \gg K_\parallel$, the growth rate becomes

$$\gamma_i(\omega_0, k, k_\parallel) = \frac{\pi}{4c_Z}\frac{\omega_{pr}^2}{\omega_{pi}^2}\frac{k^2v_A^2}{\omega_0}\exp\left[\frac{-\omega_{ce}}{(k_\parallel c - \omega_0)c_Z}\right] \tag{8}$$

to the lowest order in λ. At low frequencies the growth rate increases monotonically, and at higher frequencies we can use the whistler branch of the dispersion relation ($\omega_0 = kk_\parallel v_A c/\omega_{pi}$). The growth rate of the fastest growing wave can be obtained using the conditions $\partial\gamma_i(k_\parallel, k)/\partial k_\parallel = 0$ giving $\gamma_i(k_\parallel)$ and $\partial\gamma_i(k_\parallel)/\partial k_\parallel = 0$ giving

$$\gamma_i^{\max} = \frac{\pi}{16}\frac{\omega_{pr}^2}{\omega_{ce}}\exp(-1) = 1.3\cdot 10^{-9}\frac{n_r}{B_T} \tag{9}$$

(where B_T denotes B in Tesla) is the growth rate of the most unstable mode. Note that the dependence on electric field is solely contained in the number of runaway electrons n_r derived in Section 2. To obtain Eq. (9) we have made the following assumptions: $|k| \gg |k_\parallel|$, $\omega_{pe}^2 \gg k^2c^2 \gg \omega_{pi}^2$, $\omega_{ci} \ll \omega_0 \ll \omega_{ce}$, $k_\perp^2 v_{Te}^2 \ll \omega^2$, $\omega\omega_{ci} \ll k^2v_A^2 \ll \omega\omega_{ce}, \lambda \ll 1$ and $\alpha \gg K_\parallel$. The most unstable wave has the wave number $kv_A/\omega_{pi} = 1/2$, the parallel wave number $k_\parallel c = 2\omega_{ce}/c_Z$, and the wave frequency $\omega_0 = \omega_{ce}/c_Z$, so the assumptions are clearly satisfied.

To determine the instability threshold we must compare the growth rate with the damping due to collisions. Reference [12] shows that electron-electron collisions do not contribute to the collisional damping and ion-electron collisions can be accounted for by adding to the wave frequency an imaginary part $\omega \to \omega - i\gamma_d$, where $\gamma_d = -1.5\tau_{ei}^{-1}$. Here $\tau_{ei} =$

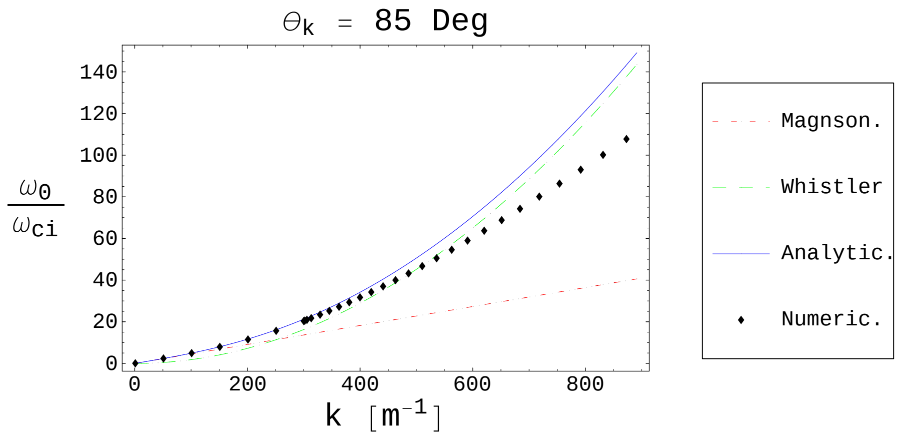

Figure 2: Comparison of numerical and analytical dispersion relations for a fixed angle of propagation ($n_e = 5\cdot 10^{19}$ m^{-3}, $B = 2$ T, $T = 10$ eV deuterium plasma).

$3\pi^{3/2}m_{e0}^2 v_{Te}^3 \epsilon_0^2/n_i Z^2 e^4 \ln\Lambda$ is the electron-ion collision time. The threshold $\gamma_k \equiv \gamma_i - \gamma_d > 0$ can be written as

$$\frac{n_r}{n_e} > \frac{Z^2 B_T}{20 T_{eV}^{3/2}}, \tag{10}$$

where T_{eV} is the background plasma temperature in eV and n_r/n_e is the fraction of the runaways. This inequality is the local threshold for the instability of the magnetosonic-whistler wave, where every quantity is to be understood at a given location.

The critical runaway fraction grows with magnetic field strength, so the magnetosonic-whistler wave is more easily destabilized for low magnetic fields. Figure 1 illustrates the threshold in plasma temperature as a function of the toroidal magnetic field strength for different runaway ratios. In this and later figures we show calculations for pure deuterium plasma ($m_i = 2m_p$, $Z = 1$).

3.2. Numerical analysis

The perturbative analysis is complemented by a numerical analysis. First, the runaway contribution to the susceptibility tensor was evaluated for relevant plasma parameters by numerically integrating expression (5) (and similar expressions for χ_{22}^r and χ_{12}^r that are not given here but can be found in [11]). As expected, $\mathrm{Re}\chi_{11}^r$, $\mathrm{Re}\chi_{22}^r$ and $\mathrm{Im}\chi_{12}^r$ have been found to be negligible compared to the background electron and ion contributions to the susceptibility tensor for all resonances and for runaway fractions up to 10^{-2}. The tensor elements are largest for $n = \pm 1$ and only the anomalous Doppler resonance ($n = -1$) contributes to the growth rate. Numerical integration of $\mathrm{Im}\chi_{11}^r$, $\mathrm{Im}\chi_{22}^r$ and $\mathrm{Re}\chi_{12}^r$ confirms that the assumptions leading to Eq. (4) are satisfied.

The results of the perturbative stability analysis are confirmed by the numerical solution of the full dispersion relation. To this end Eq. (3) has been solved with a damped Newton's method with the starting point derived from the analytical solution. In cases when this method has convergence problems a variant of the secant method was used with

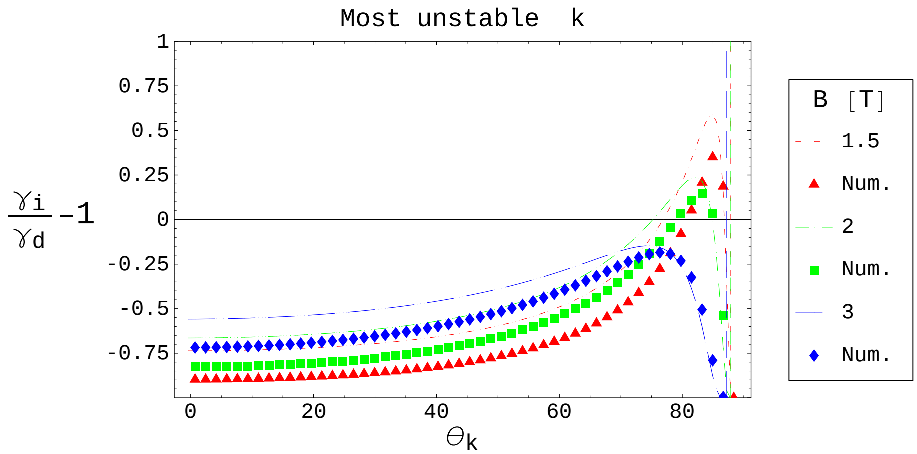

Figure 3: Numerical and analytical growth rates for deuterium plasma at different magnetic field strength values ($n_e = 5 \cdot 10^{19}$ m^{-3}, $T = 10$ eV, $n_r/n_e = 5 \cdot 10^{-3}$).

varying step lengths and linear extrapolation to determine the starting direction. The analytically derived magnetosonic-whistler dispersion relation was checked against the numerical solution of the dispersion relation excluding the runaway susceptibility term, but using the full hot plasma susceptibility [11] for both ions and electrons. Figure 2 shows the results of the analytical and the numerical dispersion relation together with the two approximations: the magnetosonic-wave dispersion for low frequency limit and the whistler-wave dispersion for the high frequency limit. The dispersion relations are plotted assuming a fixed angle of propagation ($\theta_k = 85°$). This angle will be shown to be close to the propagation angle giving the maximum growth rate for the set of plasma parameters used. The deviation of the analytical and numerical values at higher frequencies is due to the neglect of the χ_{11}^e and χ_{22}^e electron terms and the identity tensor in the dielectric tensor.

Next, we investigate the dependence of the growth rate on plasma parameters. The scaling of growth rate with respect to the magnetic field is the most interesting since experimental observations suggest that the number of runaways generated in a disruption is dependent on the magnetic field strength. Normalized growth rates as a function of propagation angle for different magnetic field strengths are presented in Fig. 3, where the threshold corresponds to $\gamma_i/\gamma_d - 1 = 0$. Growth rates calculated from the perturbative analysis, are compared to numerical solutions of the dispersion relation including the imaginary part of the most important runaway susceptibility term ($\mathrm{Im}\chi_{11}^r$) in the dielectric tensor and the full hot plasma susceptibility [11]. The vertical line at large θ_k shows the end of the range of validity of our approximation as $(1 - y)$ turns negative. Note that only waves with $|k| \gg |k_\parallel|$ are unstable. In the region of validity and for propagation angles close to perpendicular, the numerical results lie close to the analytical ones.

As expected from the analytical expression for the threshold, Eq. (10), Fig. 4 shows that the maximum normalized growth rates are not sensitive to the plasma density. For lower densities however, the maximum of the growth rate is shifted towards larger $k_\parallel$ making

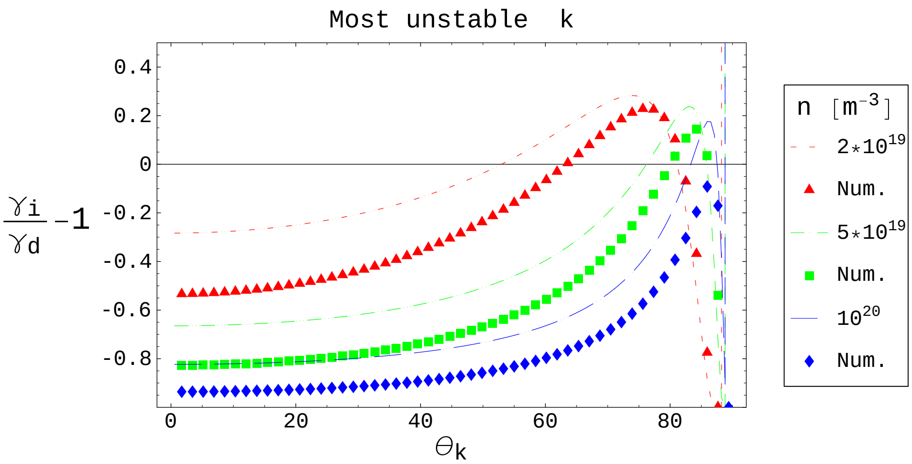

Figure 4: Analytical and numerical growth rates for deuterium plasma just above the threshold ($B = 2$ T, $T = 10$ eV, $n_r/n_e = 5 \cdot 10^{-3}$).

our assumption $|k_\parallel| \ll |k|$ invalid, and for very much higher densities the assumption $\omega_{pe}^2 \gg k^2c^2$ is violated.

Further numerical calculations showed that finite temperature effects distort the curve at very high temperatures (around a few keV depending on the density). At low post disruption temperatures the curve only changes by a multiplying constant. Higher temperatures are more unstable due to the weakness of collisional damping.

4. Quasi-linear analysis

Beyond the linear phase of the instability, the dynamics of the resonant interaction between the electrons and waves can be described by quasi-linear theory. The evolution of the distribution of the relativistic runaway electrons was derived in Ref. [10] giving

$$f(p_\perp, p_\parallel, t) = \frac{C}{(2\alpha\hat{\tau}(t) + p_\parallel)} \exp\left(\frac{(E-1)t/\tau - p_\parallel}{c_Z}\right) \exp\left(-\frac{\alpha p_\perp^2}{2(2\alpha\hat{\tau}(t) + p_\parallel)}\right). \tag{11}$$

Thus, pitch-angle scattering increases the mean perpendicular energy linearly with time. Assuming a narrow spectrum of unstable waves centered around $k_c = \omega_{pi}/2v_A \simeq 3 \cdot 10^3 n_{20}/B_T$ and $k_\parallel \simeq \omega_{ce}/c \ln\Lambda \simeq 30B_T$ and assuming that the time-evolution of the spectral energy is $W_k(t) = \frac{1}{2}T_e e^{2\gamma_k t}$, the time scale for perpendicular energy increase can be estimated to be $t = (1/2\gamma_k) \ln\left(\hat{\tau}\gamma_k m_e^2 c^3/\pi^3 e^2 T_e k_c^2\right) \simeq 3 \cdot 10^{-7}$ s, for $\gamma_k \simeq 10^8$ s^{-1}, $\gamma = 40$, $T_e = 10$ eV and $\hat{\tau} \simeq p_\parallel/(2\alpha) \simeq 0.1$.

5. Conclusions

We have analyzed the stability of magnetosonic-whistler waves in the presence of a relativistic runaway electron beam. A perturbative calculation of the growth rate agrees well with that found by a full numerical solution of the dispersion relation. The analysis is local, which is justified *a posteriori* by the sufficiently large growth rate. The threshold of the instability depends on the fraction of runaways, the magnetic field and the temperature of the background plasma. Quasi-linear analysis suggests that the main result of the instability is rapid pitch-angle scattering of the resonant electrons.

We speculate that the presence of a magnetosonic-whistler wave instability may be the reason for the observation that the number of runaway electrons produced during disruptions in large tokamaks depends sensitively on the magnetic field strength. One reason for the absence of runaways below a critical toroidal magnetic field of around 2.2 T [3, 4, 5] could be that the whistler instability scatters runaways and prevents the beam from forming. However, in order to make a more definite judgement about the importance of the latter, it would be necessary to refine the analysis performed in the present paper. In particular, a self-consistent simulation of the runaway distribution function and electric field evolution, as achieved for instance by the ARENA code [2], could be coupled to an evaluation of the instability growth rate.

Acknowledgements This work was funded jointly by the United Kingdom Engineering and Physical Sciences Research Council and by the European Communities under Association Contracts between EURATOM, UKAEA, HAS and *Vetenskapsrådet*. The views and opinions expressed herein do not necessarily reflect those of the European Commission. One of the authors (G. Pokol) acknowledges the support of a bilateral scholarship of the Swedish Institute and the Hungarian Scholarship Board and a grant of the System International Foundation.

References

[1] M. N. Rosenbluth, S. V. Putvinski, Nuclear Fusion, **37**, 1355, (1977).

[2] L.-G. Eriksson, P. Helander, F. Andersson, D. Anderson, and M. Lisak, Phys. Rev. Lett. **92**, 205004 (2004).

[3] R. D. Gill, B. Alper, M. de Baar et al, Nuclear Fusion, **42**, 1039 (2002).

[4] R. Yoshino, S. Tokuda, Y. Kawano, Nuclear Fusion, **39**, 151, (2000).

[5] M. Lisak, U. Schneider, G. Martin et al. Nuclear Fusion, **42** 937 (2002).

[6] V. V. Parail and O. P. Pogutse, Nuclear Fusion, **18**, 303 (1978).

[7] V. V. Parail and O. P. Pogutse, Reviews of Plasma Physics, 11, 1 (1986).

[8] C. S. Liu and Y. Mok, Phys. Rev. Lett, **38**, 162, (1977).

[9] M. N. Rosenbluth, P. B. Parks, D. Post, S. Putvinski, N. Putvinskaya, H. A. Scott, Proc. 16th IAEA Fusion Energy Conf. Montreal, 1996, Vol. 2, IAEA, Vienna, IAEA-CN-64/FP26, 979 (1997).

[10] T. Fülöp, G. Pokol, P. Helander and M. Lisak, Physics of Plasmas, **13**, 062506, (2006).

[11] T. H. Stix, Waves in plasmas, American Institute of Physics, New York, 1992.

[12] M. Brambilla, Phys. Plasmas, **2**, 1094, (1995).

[13] J. A. Wesson, R. D. Gill, M. Hugon et al., Nuclear Fusion **29**, 641 (1989).